DOI 10.1515/aee-2015-0045

Active suspension system with integrated electrical tubular linear motor: design, control strategy and validation

Andreas Thul, Daniel Eggers, Björn Riemer, Kay Hameyer

RWTH Aachen University
Institute of Electrical Machines
Chair of Electromagnetic Energy Conversion
Schinkelstr. 4, Aachen, Germany

e-mail: andreas.thul@iem.rwth-aachen.de

(Received: 10.09.2015, revised: 20.09.2015)

Abstract: This paper focuses on the design and control of an active suspension system, where a tubular linear motor is integrated into a spring damper system of a vehicle. The spring takes up the weight of the vehicle. Therefore the electric linear motor can be designed very compact as it has to provide forces to adjust the damping characteristic only. Design and construction of the active suspension system, a control strategy and validation measurements at a test bench are presented.

Key words: active vehicle suspension, tubular linear electric drive, electric motor control

1. Introduction

The traveling comfort of automobile vehicles depends on the behavior of the vertical suspension system. Usually a combination of a mechanical spring and a hydraulic damper is used. Although hydraulic dampers allow some adjustment in their force reaction to a movement, a wide change can only be achieved by choosing another damper-spring combination. Hence the behavior is fixed for a particular vehicle. Adjustments during operation in order to optimize traveling comfort requires a suspension system, where the provided force can be actively set. It is possible use a rotating electric motor as active component [1, 2], but this requires an additional gear to transform the torque to a linear acting force. A linear electric drive would be a more suitable active component, since it can be easily controlled and allows fast dynamic force changes. A pure electric system is not feasible because electric motors only deliver forces when currents are present. Thus a hybrid topology similar to the approach described in [3] and [4] is chosen, where the electric motor is connected in parallel to a conventional damper and spring. So the linear drive can adjust the system behavior by providing comparatively small propulsive forces. This allows to design a linear motor which can be integrated in the conven-

tional system, thus no extra space is needed for the motor. Compared to existing active damping systems, a simpler integration in the vehicle body is possible since no further adjustments to the body are necessary [5].

Chapters two and three describe the motor design and the control strategy, as presented in [6]. Afterwards, the validation on the test bench and additional measurements are shown.

2. Design of the actor concept

The design has to deal with the conflict of an easy to assemble topology for series production on the one hand in line with high performance to guarantee a good ride comfort on the other hand. So the electric actuator consists of a cylindrical rotor and stator, which are arranged concentrically to each other. The air gap between rotor and stator is $\delta = 1$ mm, which allows a relative tilt movement of these components to each other without damage. The stator is made of a massive, tubular ferromagnetic material. The slots for the coils, which are three-phase interconnected, are milled in the stator unit. As shown in Figure 1, each coil of a phase is connected in series. The linor is constructed of soft magnetic laminated sheets that are stacked and braced. The basic magnetic excitation is performed by surface mounted neodymium magnets, which are glued and bandaged. The linor contains four pole pairs, each pole pair connected to three stator teeth.

Due to the mechanical spring and the oil damper, the complete damping system remains functional during an interruption of the power supply.

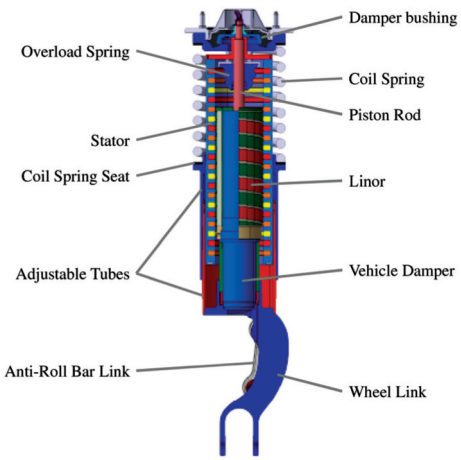

Fig. 1. Overview of the designed damping system [5]

Due to the limited volume of the construction space and the required mechanical strength of the entire system a solid material has to be chosen for the stator. This results, compared to a laminated construction, in barrier-free eddy current paths in the stator which leads to higher eddy current losses in operating points. Since the Energy is generated by the mechanical move-

ment, the eddy currents lead to an additional contribution to the damping. This damping force component will still be present, if the motor is not electrically operated.

The stator is made of two half shells of the material ST27, which was chosen because of it machining properties. On behalf of this geometry the coils are easy to insert into the stator slots. Those coils are designed as concentrated windings because a distributed or helical winding yields no significant advantage in comparison to production effort.

Based on an operational profile the maximum propulsive force has been identified to F_{max} = 2 kN and the maximum mechanical frequency to F_{max} = 30 Hz as well as the maximum linor travel length of s = +60 mm and s = –80 mm. Due to the limited construction space, the entire suspension unit has been limited to an outer diameter of D_o = 150 mm and the maximum length of l = 320 mm. For the integration of the actuator in the high voltage circuit of the automobile, the maximum voltage is defined to U_{max} = 320 V.

First, the general concept of the hybrid damping system is examined. The system contains three main components: a hydraulic oil damper, a mechnanical spring and the linear electric motor. Two different types of springs have been considered, an externally mounted torsion bar spring and a coil spring, which can be integrated in the damping system. The torsion spring allows a maximum outer diameter of the stator of $D_{o,tor}$ = 150 mm, in the configuration with the coil spring this parameter is reduced to $D_{o,coil}$ = 108 mm. Due to the oil damper, the inner diameter of the linor is determined to D_i = 57 mm in both cases. The linor is mounted directly to the surface of the oil damper.

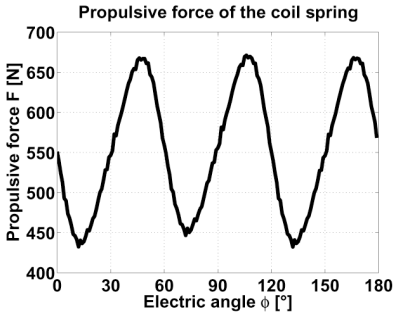

Fig. 2. Maximum propulsive force for the actuator with coil spring

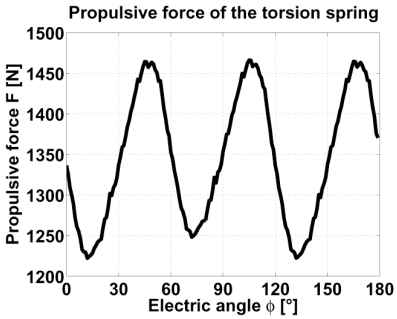

Fig. 3. Maximum propulsive force for the actuator with torsion bar spring

The maximum propulsive force for the two concepts is shown in Figure 2 and 3. The propulsive force is determined by static simulations of a 2D axisymetric Finite Element model of the actor. For both geometries a peak-to-peak cogging torque ripple of $\Delta F_{cog} \approx 250$ N is identified. The average propulsive force for the torsion bar spring concept is $F_{tor} \approx 1350$ N (Fig. 3), for the coil spring concept the force is reduced to $F_{coil} \approx 550$ N (Fig. 2) due to the smaller construction space.

To increase the riding comfort, the cogging torque ripple has to be reduced. For this, a skewing of the permanent magnets by a one slot pitch is considered. Figure 4 shows the structure of the linor with skewed permanent magnets. The permanent magnets are applied on the linor in 20° steps. The FE simulations are carried out using the multi-slice method [7].

Figures 5 and 6 show the propulsive force for both spring concepts. The results show a reduction of the cogging force ripple to $\Delta F_{cog,coil} = 5$ N and $\Delta F_{cog,tor} = 8$ N peak-to-peak. A disadvantage of the homogenisation of the propulsive force is the reduction of the mean force to $F_{tor} \approx 1117$ N (Fig. 6) as well as $F_{coil} \approx 460$ N (Fig. 5).

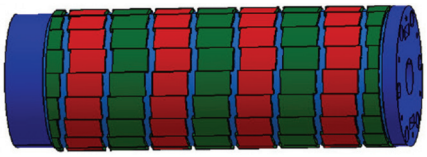

Fig. 4. Linor with skewed permanent magnets

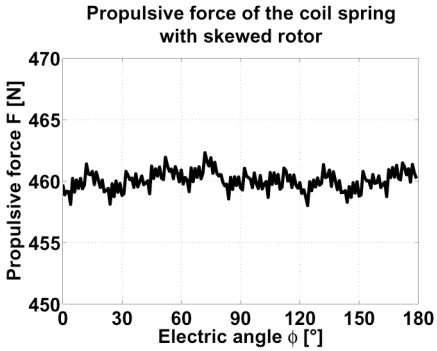

Fig. 5. Propulsive force for the coil spring concept with skewed rotor

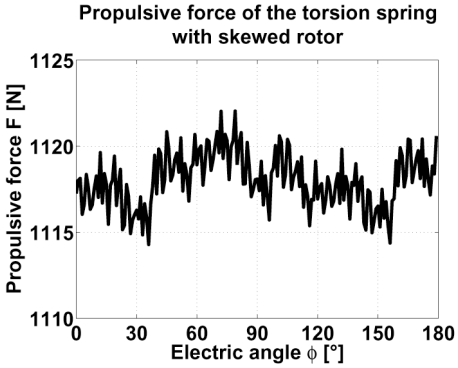

Fig. 6. Propulsive force for the torsion bar spring concept with skewed rotor

The torsion bar spring concept leads to higher propulsive forces of the linear motor, since more stator volume is available. But the external spring would require significant changes to the car body, thus the coil spring concept, where all components are integrated in one part, is chosen.

3. Motor control

For a fast dynamic behavior, a field-oriented control scheme is implemented. The controller structure is shown in Figure 7. First, the inner current control loop is described. The outer force control is designed afterwards.

The electrical model of the actor is described by the voltage equations in the field-oriented dq reference frame [8]:

$$u_d = R \cdot i_d + L \cdot \frac{di_d}{dt} - \omega_{el.} \cdot L \cdot i_q \tag{1}$$

and

$$u_q = R \cdot i_q + L \cdot \frac{di_q}{dt} + \omega_{el.} \cdot \left(\Psi_F + L \cdot i_d\right), \tag{2}$$

R, L and Ψ_F denote stator resistance, stator inductance and permanent magnet flux linkage, respectively. The model parameters have to be identified for the controller design. Therefore the spring is removed and the damping system is coupled to a hydraulical linear actuator. The stator resistance R is measured by feeding a dc current into the winding at standstill. The permanent magnet flux linkage and the stator inductance L can be determined by a no load pulling test and a continued short circuit test, respectively. The limited linor moving range requires some adjustments compared to a rotating machine. The no load test has to be performed with constant linor speed and the acceleration to reverse the travel direction has to be kept small. Therefore a comparatively small mechanical speed is chosen, the measured line-to-line voltage is shown in Figure 8.

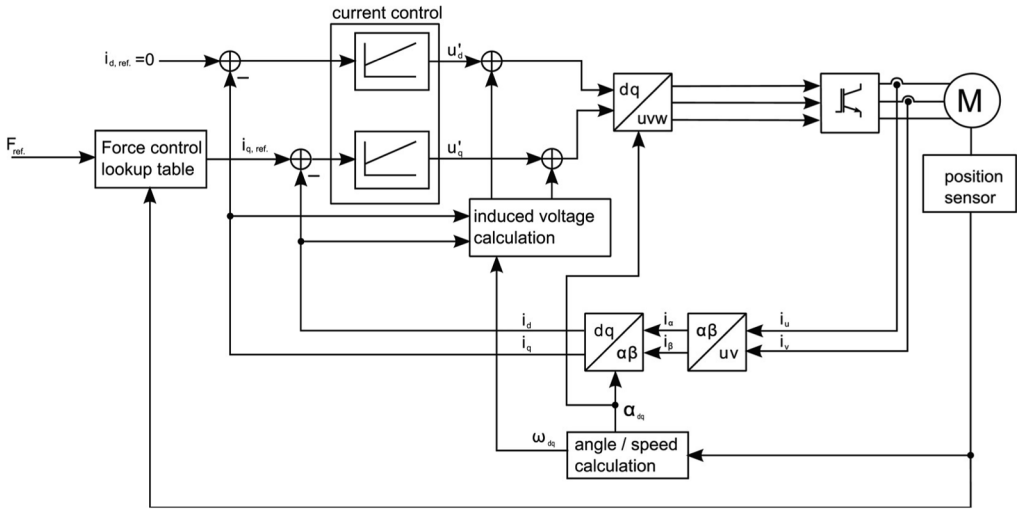

Fig. 7. Electric motor control structure

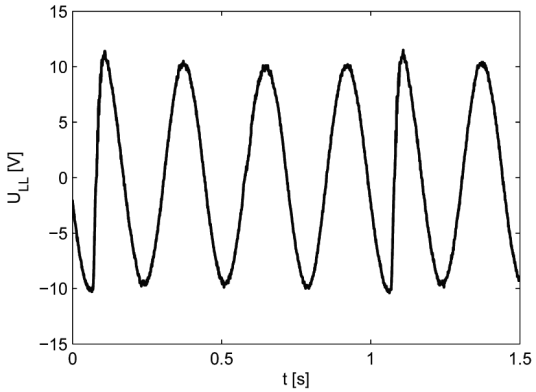

Fig. 8. Induced voltage measured for a rectangular speed profile (amplitude 42.5 mm/s, frequency 1 Hz)

The induced voltage is distorted at the reversing points, but unaffected during the travel with constant speed. Thus the peak voltage value is taken from the undistorted travel period and the flux linkage can be calculated:

$$\Psi_F = \frac{\hat{u}_{line} \cdot \tau_p}{\sqrt{3} \cdot v}. \tag{3}$$

The short circuit test is usually carried out at higher speeds to eliminate the influence of the stator resistance. But here the the travel length is too small, thus a steady state cannot be reached at higher speed values. The measurement is carried out at low speed instead to ensure that a steady state is reached during the linor travel. The inductance L can now be calculated

from (1) by choosing u_d and the derivative of i_d to zero. The identified parameter values are summarized in Table 1.

Table 1. Identified motor parameters

Motor parameter		**Value**
Stator resistance	R	2.4 Ω
Inductance	L	8.2 mH
Permanent magnet flux linkage	Ψ_F	0.2585 Vs

Since the linor magnets are mounted on the surface, there is no significant reluctance torque to be expected and the direct current set point is thus always zero. The induced voltages are calculated from the measured currents and used as feed forward control signals to linearize the system:

$$u'_d = R \cdot i_d + L \cdot \frac{di_d}{dt} \tag{4}$$

and

$$u'_q = R \cdot i_q + L \cdot \frac{di_q}{dt}. \tag{5}$$

For the feedback path PI controllers are used. The controller reset times are set equal to the electrical time constant to compensate the model pole. The gain is chosen experimentally by evaluating the step response during standstill. Figure 9 shows the measured quadrature current for a choice of $k_{PI} = 5\ R$. The chosen value leads to a fast response without overshoots. Afterwards, a measurement with a sinusoidal reference current is carried out. Here, a frequency of $f = 1$ Hz was chosen. As seen in Figure 10, the controller can impress a sinusoidal current as well.

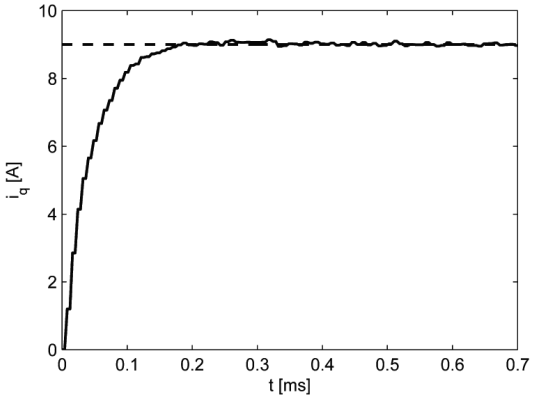

Fig. 9. Step response of the current controller

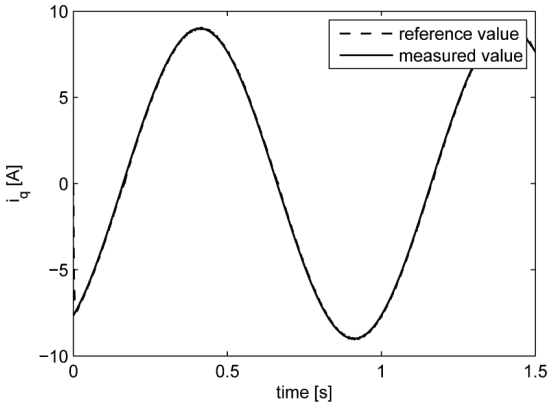

Fig. 10. Controller performance for sinusoidal reference currents

4. Validation

First, the behavior of the current control in the frequency domain is analysed. Therefore the linor is fixed and harmonic reference currents with different frequencies are impressed. From the measured and reference current values the transfer function is calculated. Figure 11 shows frequency response of the current transfer function at different linor positions. The systems has a low pass characteristic. The cutoff frequency is high enough to guaranty a small damping of the magnitude ratio in the operating frequency range.

For further validation additional measurements during movement are taken. The linor is sinusoidally moved by a hydraulic actor with a position amplitude of 25 mm and a frequency of 0.8 Hz.

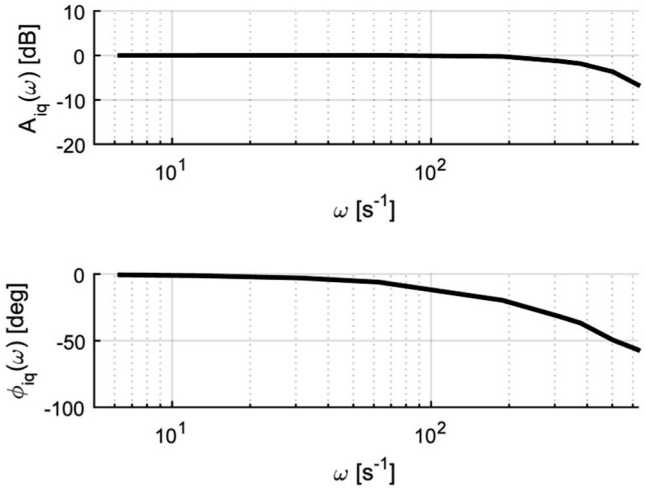

Fig. 11. Frequency response for the current transfer function

Figure 12 shows the results for a constant reference quadrature current. The mechanical position amplitude is increased and decreased sinusoidally at start up and end of the measurement to avoid high oil pressure peaks in the hydraulic system. The same experiment was then repeated with a sinusoidal reference current, as shown in Figure 13. The results indicate that the current controller performance is not affected. Since for the moving measurements the reference current frequency is increased to 30 Hz, a higher phase delay between reference and actual current is observed than in Figure 10. This could be compensated by a faster controller setting, since further measurements indicated that a stable operation would still be possible with increased controller gains.

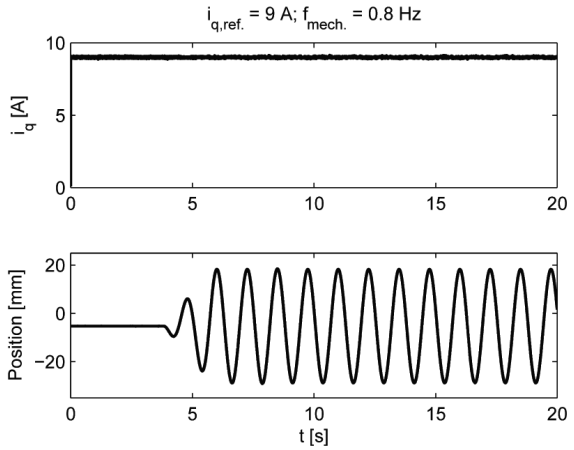

Fig. 12. Controller performance at constant reference current during movement

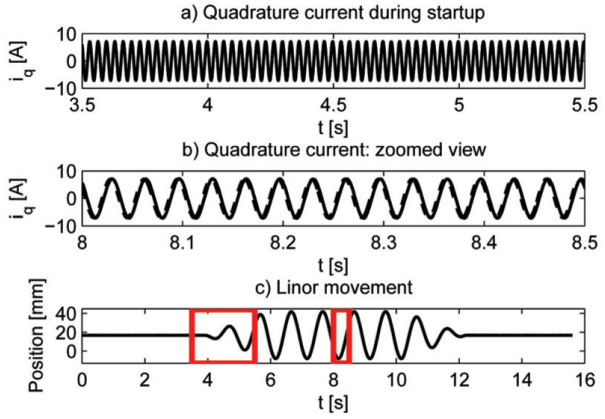

Fig. 13. Controller performance at sinusoidal reference current during movement start up (a) and steady-state (b). The shown time intervals are highlighted in the position trajectory plot (c)

The motor force could be controlled by an outer feedback loop, but in the combined actor only the overall force is measurable, which contains components generated by linear motor,

hydraulic damper, friction in the case bearing and the inertia of the moving parts. Due to the nonlinear behavior of damper and friction forces, a separation of the motor force is complex. Therefore a feed-forward control scheme is implemented instead. In a first step, a static test bench shown in Figure 14 is used to identify the propulsive motor force.

The coil spring is removed and a manual spindle drive allows to change the linor position. During the measurements the linor is at standstill, thus the damper does not generate any force and the motor force can be measured directly. The force is measured for different positions and quadrature currents, the results are shown in Figure 15. With the acquired data a control matrix can be generated, which contains the reference current for different linor positions and force command values. With the control matrix, the difference between measured and reference force was limited to 10 %, as shown in Figure 16.

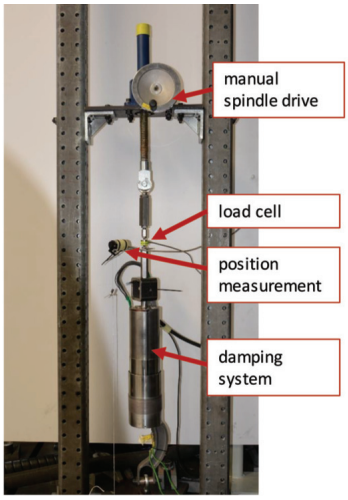

Fig. 14. Testbench for force measurements

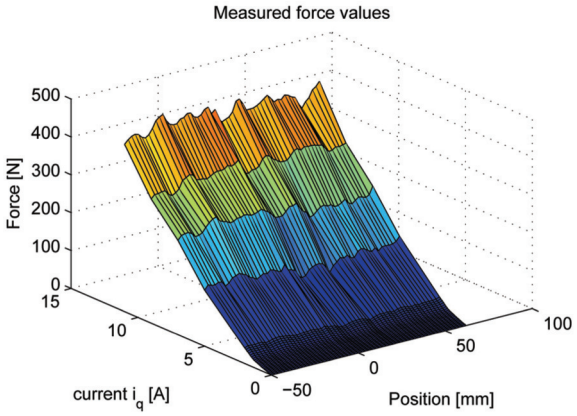

Fig. 15. Measured force for different positions and reference quadrature currents

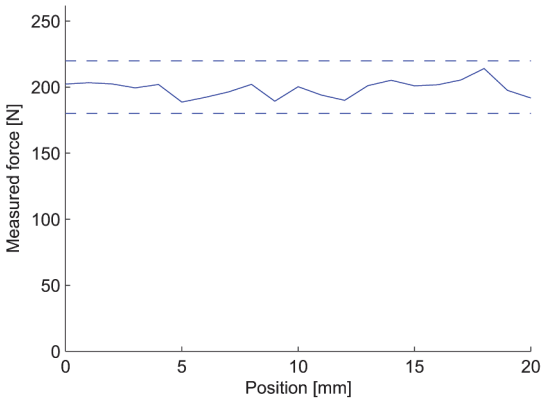

Fig. 16. Measured force with force control lookup table

5. Conclusions

For an active automobile suspension system a compact electric linear motor with skewed permanent magnets is designed. By impressing an additional force the designed actuator is able to change the behavior of the damping system. The functionality of the field oriented control is validated by measurements at standstill and during linor movement. A feed forward force control strategy is designed based on force measurements on the testbench.

In a future work, the damping system can be mounted in a testbench setup containing additional parts of the vehicle suspension. Furthermore, the system can be tested in an actual vehicle.

Acknowledgements

The authors would like to thank Gerrit Schellstede and Michael Klein of the Institute for Automotive Engineering, RWTH Aachen University, for their help with building the test bench and conducting the measurements. The project was financially supported by the German Federal Ministry of Education and Research (FKZ: 13N10656) and the RWTH Aachen University Innovation Funds.

References

[1] Kraus M., *Elektromechanische Aktuatorik – Potentiale für Hinterachskinematik.* Automobiltechnische Zeitschrift (ATZ) 111(9):. 636-642 (2009).

[2] Münster M., Mair U., Gilsdorf H. et al., *Elektromechanische aktive Aufbaukontrolle.* Automobiltechnische Zeitschrift (ATZ) 111(9): 644-649 (2009).

[3] Gysen B., Paulides J., Janssen J., Lomonova E., *Active Electromagnetic Suspension System for Improved Vehicle Dynamics.* IEEE Trans. Veh. Technol. 59(3): 1156-1163 (2010).

[4] Gysen B., Janssen J., Paulides J, Lomonova E., *Design Aspects of an Active Electromagnetic Suspension System for Automotive Applications.* IEEE Trans. Industry Applications 45(5): 1589-1597 (2009).

[5] Klein M., Eckstein L., *Development Tool for the Optimization of Vertical Dynamics in Chassis Development.* Chassis.tech plus (2012).

[6] Thul A., Eggers D., Riemer B., Hameyer K., *Design and control of an active suspension system with integrated electrical tubular linear motor.* 10th International Symposium on Linear Drives for Industry Applications, Aachen (2015).
[7] Schmülling B., Leßmann M., Riemer B., Hameyer K., *The multi slice method for the design of a tubular linear motor with a skewed reaction rail.* Proc. Conf. 18th International Conference on Electrical Machines (2008).
[8] Schröder D., *Elektrische Antriebe – Regelung von Antriebssystemen*. Springer Verlag, Berlin Heidelberg (2009).